Norsk institutt for luftforskning
Norwegian Institute for Air Research

Iceland Liechtenstein Norway grants

Review of methods that can be used in the assessment of atmospheric deposition

Wenche Aas, Joana Soares, Paul Hamer,
Philipp Schneider, Tove Svendby and Cristina Guerreiro

NILU report 33/2022

NILU report 33/2022	ISBN: 978-82-425-3108-7 ISSN: 2464-3327	CLASSIFICATION: A – Unclassified (open report)
DATE 08.05.2023	SIGNATURE OF RESPONSIBLE PERSON Aasmund Fahre Vik (sign.) Deputy director and CTO	NUMBER OF PAGES 34
TITLE Review of methods that can be used in the assessment of atmospheric deposition		PROJECT LEADER Cristina Guerreiro
		NILU PROJECT NO. O-120159
AUTHOR(S) Wenche Aas, Joana Soares, Paul Hamer, Philipp Schneider, Tove Svendby and Cristina Guerreiro		QUALITY CONTROLLER Cristina Guerreiro
REPORT PREPARED FOR The State Treasury – Chief Inspectorate for Environmental Protection (GIOS) Bitwy Warszawskiej 1920 r. 3, PL-02-362 Warsaw, Poland Department of the Environmental Monitoring Al. Jerozolimskie 92, PL-00-807 Warsaw, Poland		CONTRACT REF. Barbara Toczko, b.toczko@gios.gov.pl

ABSTRACT

There are three main approaches for estimating the atmospheric deposition: 1) From measurements of air and precipitation chemistry combined with statistical interpolation, 2) Chemical transport models, 3) Combined observations and atmospheric model calculations. This report reviews these different approaches and come with some general recommendations on the different strategies and the way forward for Poland.

The report was made for the project "Strengthening of atmospheric deposition assessment in Poland based on Norwegian experience" under the program "Environment, Energy and Climate Change", financed by the European Economic Area Financial Mechanism 2014-2021".

NORWEGIAN TITLE

Gjennomgang av metoder som kan benyttes for å beregne atmosfærisk avsetning

KEYWORDS

Atmospheric deposition | Geostatistics | Chemical transport models

ABSTRACT (in Norwegian)

Det er tre hovedtilnærminger for å estimere atmosfæriske avsetningen: 1) Fra målinger av luft- og nedbørskjemi kombinert med statistisk interpolasjon, 2) kjemiske transportmodeller, 3) kombinere observasjoner og atmosfæriske modellberegninger. Denne rapporten gjennomgår disse forskjellige tilnærmingene og kommer med noen generelle anbefalinger om de forskjellige strategiene og veien videre for Polen.

Denne rapporten ble laget for prosjektet "Strengthening of atmospheric deposition assessment in Poland based on Norwegian experience" under programmet "Environment, Energy and Climate Change", finansiert av European Economic Area Financial Mechanism 2014-2021".

PUBLICATION TYPE: Digital document (pdf)	COVER PICTURE: Source: NILU

Citation: Aas, Wenche, Soares, J., Hamer, P., Schneider, P., Svendby, T. and Guerreiro, C. (2022). Review of methods that can be used in the assessment of atmospheric deposition. (NILU rapport 33/2022). Kjeller: NILU.

NILU's ISO Certifications: NS-EN ISO 9001 and NS-EN ISO 14001. NILU's Accreditation: NS-EN ISO/IEC 17025.

Contents

Review of methods that can be used in the assessment of atmospheric deposition

Introduction

Maps of atmospheric deposition of pollutants are critical in estimating the environmental impacts of pollution on ecosystems at risk (Fu et al., 2022). There are three different approaches for estimating the atmospheric deposition:

1) From measurements of air and precipitation chemistry combined with statistical interpolation
2) Chemical transport models (CTMs)
3) Combined observations and atmospheric model calculations, often called data assimilation or data-model fusion.

Under each of these categories there is a range of different approaches and methods. This report includes a review showing examples of results and comparison of methods for deposition calculation for some selected compounds. The focus will be on inorganic components (sulfur, nitrogen) and trace elements (cadmium, lead) since there is more data available for these. Persistent organic pollutants (POPs) will be also discussed briefly.

The three approaches have different strengths and weaknesses, and they may complement each other. There are two main limitations with the statistical interpolation method (1). Firstly, having enough representative sites to cover the whole region. Very often there are large areas where there are no sites available causing large uncertainty in the interpolation between the sites. Secondly, the dry deposition is hardly measured directly, and it is necessary to estimate the deposition velocities based on literature or use modelled data. In this report we will mainly focus on precipitation data (wet deposition) when presenting the statistical interpolation techniques. Though one chapter discuss how interpolation of air concentrations are done in EEA.

The CTMs (2) usually have a much higher spatial and temporal coverage and can potentially fill the gaps in the observational based method. CTM capabilities have improved in the last decades, however, there remain large uncertainties in CTM simulations due to incomplete knowledge of emissions and in the chemical schemes, and other sources of uncertainty. How large these uncertainties are dependent on which compound in question. It is critical to have sufficient number of observations that can validate the model output, though it is difficult to validate the dry deposition fluxes since these are scarcely measured, as also stated above. In this report the dispersion models developed under the Co-operative programme for monitoring and evaluation of long-range transmissions of air pollutants in Europe (EMEP) has been included. Some other models are briefly presented as well.

Using observations to correct modelling results (3) have a great potential to improve the estimates of the atmospheric deposition. The common approach is that the model results are adjusted by the observations giving large weight to the observed values close to stations while using the modelled values in areas with no observations. There is various way of implementing measurement model fusion, here we will present some examples of techniques used.

1 Estimate wet deposition from observation

In Poland there are observations of concentrations in precipitation at 22 monitoring sites. In addition, there are data available from 3 EMEP sites. Further precipitation heights for 162 precipitation stations can be used for better spatial information of the precipitation amount in Poland. The input data was given as monthly mean concentrations was aggregated to volume weighted annual concentration presented in Figure 1. Only a selection of the available compounds is used in this analysis to illustrate methods that can be applied.

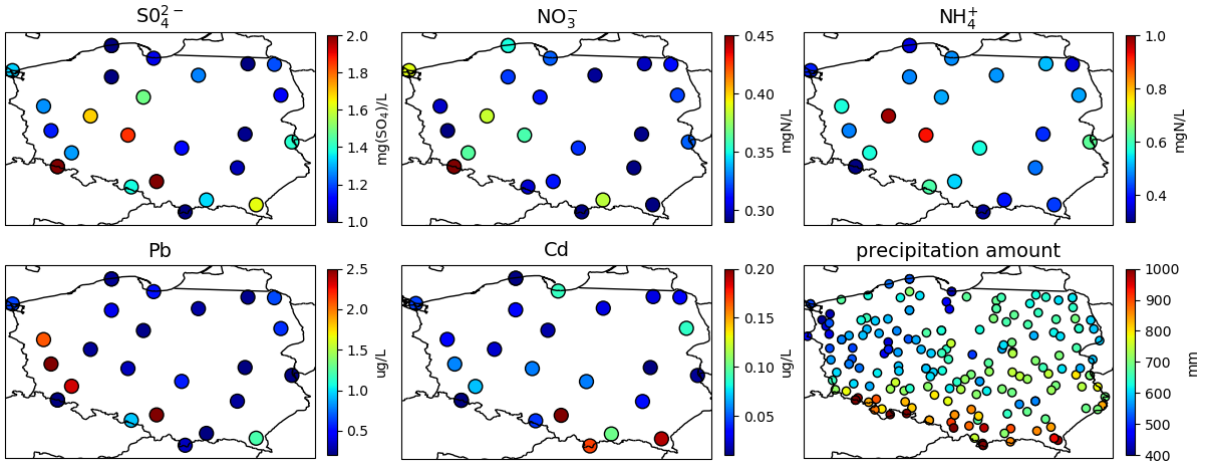

Figure 1: Annual volume weighted mean concentrations of SO_4^{2-}, NO_3^-, NH_4^+, Pb, Cd in precipitation in 2020 from the Polish national monitoring networks and EMEP.

When having observation at various locations one can use spatial statistics models to analyse the correlation between nearby points and from this deduce a spatial concentration field. There are several spatial models that can be used, such as, multiple linear regression (MLR), geographically weighted regression (GWR), inverse distance weighting (IDW) and kriging, and sometimes a combination of these. For kriging, there are several methods and approaches, like ordinary kriging (OK), regression kriging (RK), universal kriging (UK). The most used method is OK, but the choice of which kriging to use depends on the characteristics of the dataWe will not present the theory behind kriging in this report, there are several textbooks and peer reviewed papers describing the concept and the different approaches, limitations etc. The method was originally developed for geostatistical purposes (Matheron, 1963).

IDW is a very good approach for exploring spatially dense datasets and has a faster processing time for large data sets compared to kriging, and it is commonly used i.e., in forecast techniques. Kriging is a more complex approach since it explicitly takes into account the spatial autocorrelation structure of the underlying data, though one of the most used interpolation techniques and in many cases make more accurate predictions compared to other methods (Khosravi et al, 2018; Olivier and Webster, 2014), though there are several uncertainties implicit in the kriging methods which may induce errors in the interpolation if not evaluated carefully. The accuracy in any spatial interpolation techniques is highly dependent on the number of data points, their representativity and spatial correlation. In contrast to other spatial interpolation techniques such as IDW, kriging always provides an uncertainty estimate of the interpolated result.

In Norway OK has been used since 1980 to estimate atmospheric deposition (Aas et al, 2017) of inorganic components, and similar method have here been applied to the Polish observations in precipitation and compared to IDW (see Chapter 1.2).

1.1 Define an appropriate setup for kriging

In principle in geospatial correlations, things that are closer are more alike than things farther apart. In our case this can be understood as the deposition of air pollution at regional representative sites is dependent on their distance to the emission sources.

There are generally two main steps in the kriging procedure 1) Fit a variogram model to the data. 2) krige the data according to the variogram. A variogram is a model fitted to the data to describe the spatial autocorrelation between the observations. In a variogram plot, the distance between the points (observations) are related to how much the sites are correlated, illustrated in Figure 2. The x-axis represents the distance between pairs of points, and the y-axis represents the calculated value of the variogram, where a greater value indicates less correlation between pairs of points.

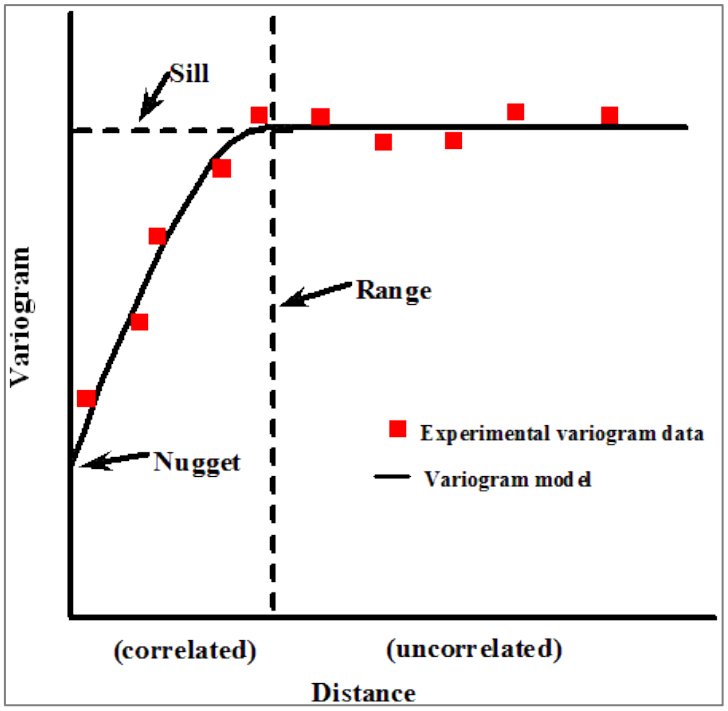

Figure 2: Theoretical illustration of a variogram plot (Copied from https://vsp.pnnl.gov/help/Vsample/Kriging_Variogram_Model.htm).

An important factor which needs to be in place for the kriging method to work properly is that the spatial variation (the correlations between stations) is statistically homogeneous throughout the surface. Though the variability may not be same in all spatial direction, so called anisotropy. If so, one should apply an anisotropic variogram model which is a function of both distance and direction.

There are several tools that are available for doing kriging. In this case we have used the R programming language and the gstat package (Pebesma, E.J., 2015; Gräler et al.,2016) or kriging and autofitVariogram from the automatic interpolation package automap (Hiemstra et al, 2008) applied on the Polish precipitation data for 2020 (see Annex 1 for the code used).

There are several parameters that control the fit of the variogram model and depending on which tools used for calculating the variogram several of these can be constrained. In the autofitVariogram in R there one can fix the three variogram parameter nugget, sill and range to a certain value as well as the model type used:

- The nugget is the y-intercept of the variogram (Figure 2). The nugget represents the small-scale variability of the data. A portion of that short range variability can be the result of measurement error. Theoretically the origin the variogram value should be zero.
- The range is the distance after which the variogram levels off (Figure 2), in other words the distance after which data are no longer correlated.
- The sill is the variance level where the variogram flattens off (Figure 2), which equal the sum of variance contributions the modelling.
- Model type. There are five different types of models that are often used: Spherical (Sph), exponential (Exp), gaussian (Gau), Matern family (Mat) and M. Stein's parameterization (Ste). The model influences the prediction of the unknown values, particularly the shape of the curve near the origin differs significantly between the models. The steeper the curve near the origin, the more influence the closest neighbours will have on the prediction.

Firstly, the kriging was done with automatic settings in the autofitVariogram, thus no constrains, top panel in Figure 3. The variograms for the five different components are very different, resulting in spatial concentrations fields which are obviously biased when comparing with the observed concentrations at the sites.

When looking at NH_4^+ and Cd which has most normal variogram plots, i.e. resemble the theoretical variogram shown in Figure 2, the curve level off around 4. This equals about 200km (4x 50km grid) which is reasonable considering the potential for long range transport of these pollutants. Variograms should move towards zero, and one should constrain the nugget to be able to get a curve which resembles a normal variogram model.

Constraining the range to 4 or nugget to 0, we get other results than no constrain, but neither are very good, panel 2 and 3 in Figure 3. The concentrations are not spatially distributed in accordance to what one expect from the observational data. However, when constraining both the nugget and the range the variogram model seems to fit better and give spatial distributions which looks reasonable, bottom panel in Figure 3.

Constraining the model type does not make a big difference, thus we let the autofitVariogram function choose the best fitting type of model. Except for NH_4, which has a Sph model, the variogram models are Ste.

We did not try to constrain the sill since that varied a lot between the different compounds. This could be considered when difficult to find a reasonable model fit. Further, possibly anisotropy in the variogram has not been assessed. This could potentially be important for some components.

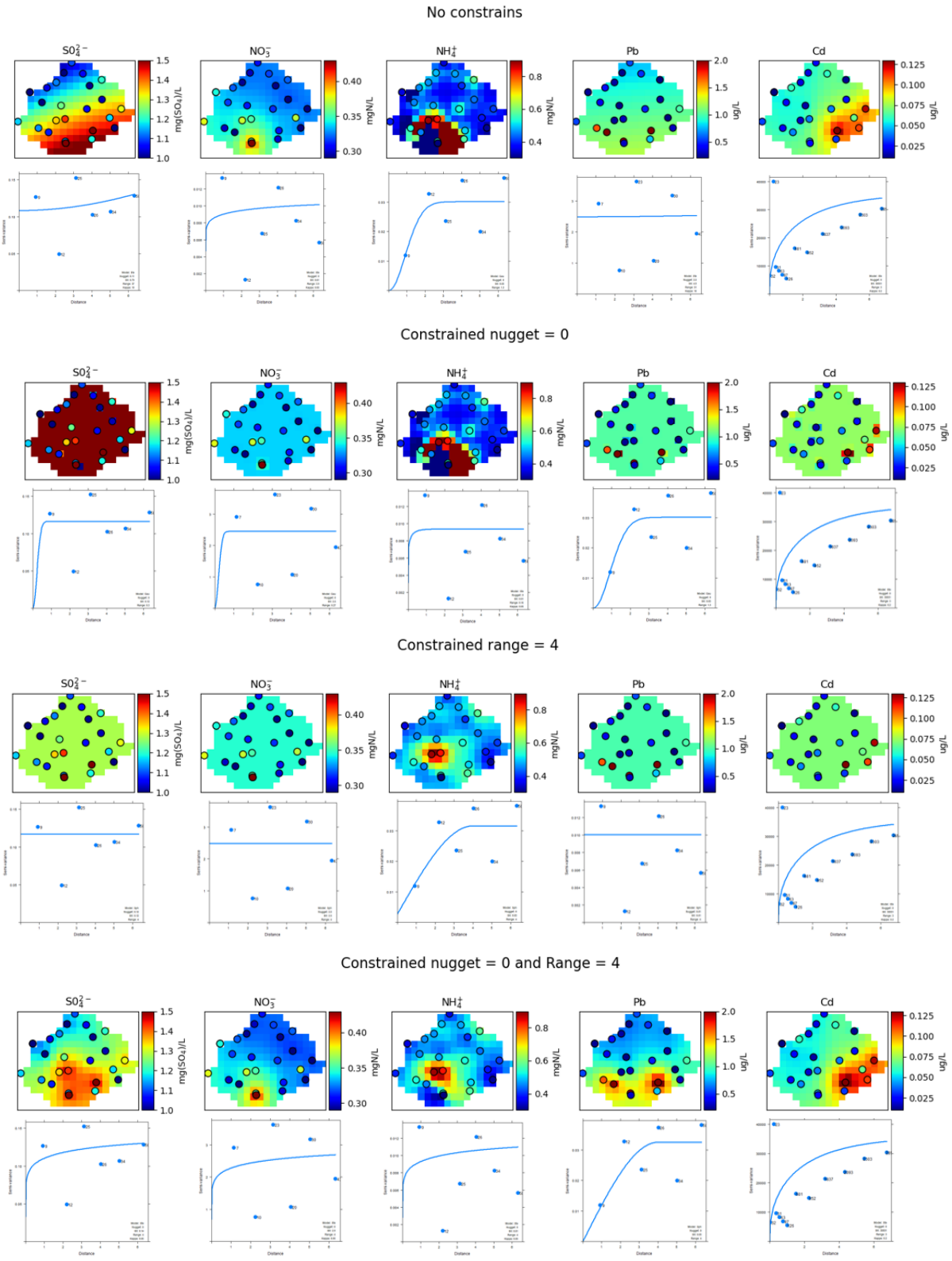

Figure 3: Testing different constrains on the variograms and the kriging results.

The example above shows that the data used do not give very reliable results without constraining the model. Several factors affect the reliability of the experimental variogram. For the case here it is especially two main issues:

- Enough sampling points. In general, the more data you have the greater is the accuracy. If too few data it is impossible to get reliable results. I.e., if the interval is larger than the correlation ranges the empirical variogram will be flat thus all the variation occurs within a shorter distance than between the sites and the model cannot be used for predicting the spatial distribution.
- Representativity of the sampling points. Outliers can cause serious distortions in geostatistics and difficulties in getting correct fit with the variograms.

When the variograms and/or kriging results do not seem reasonable one needs to check if the input data are correct or should be taken out. The kriging results are based on the input data in Figure 1 and there is obviously inconsistency at a few places. Figure 4 shows that there are obviously two places were adjacent sites are very different. This can be due to topographic reasons, local sources, or contaminations. These data need to be evaluated and changed or deleted to improve the variogram model thus more reliable kriging results.

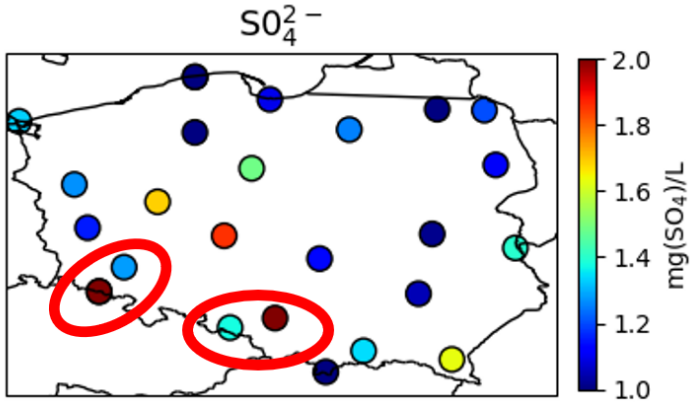

Figure 4: Annual concentration of sulfate in precipitation in Poland in 2020 highlighting sites which are inconsistent.

One should also look carefully at other years to get a best understanding of what are normal results. In the examples above we have used same constrains for all the compounds. This is not necessarily correct but simplified to illustrate the procedure.

One should also include the statistics evaluation of the variance and the spatial prediction errors to better evaluate if the best variogram model to use.

1.2 Compare interpolation techniques

The ordinary kriging (OK) with the constrains nugget=0 and range = 4, as described in Chapter 1.1 has been compared inverse distance weighting (IDW) for SO_4, NO_3, NH_4, Cd, Pb and precipitation amount (Figure 5).

The OK and IDW maps look quite similar, though there are some general differences. The IDW maps have higher concentrations around the points than seen in the OK maps, especially if neighbouring sites have very different concentration levels. This is because IDW is an exact interpolator whereas kriging-based methods are only exact if the nugget is equal to zero, which does not seem to be the case here, though we have forced the model with nugget = 0. For precipitation amount there are much

higher number of sampling points and there are not those big discrepancies in neighbouring sites causing very similar results for all the three methods.

One should compare the statistics evaluation of the variance, the spatial prediction errors to better evaluate if the models show reasonable results and if not where are the main uncertainties. Can be some regions which are more difficult to map than others.

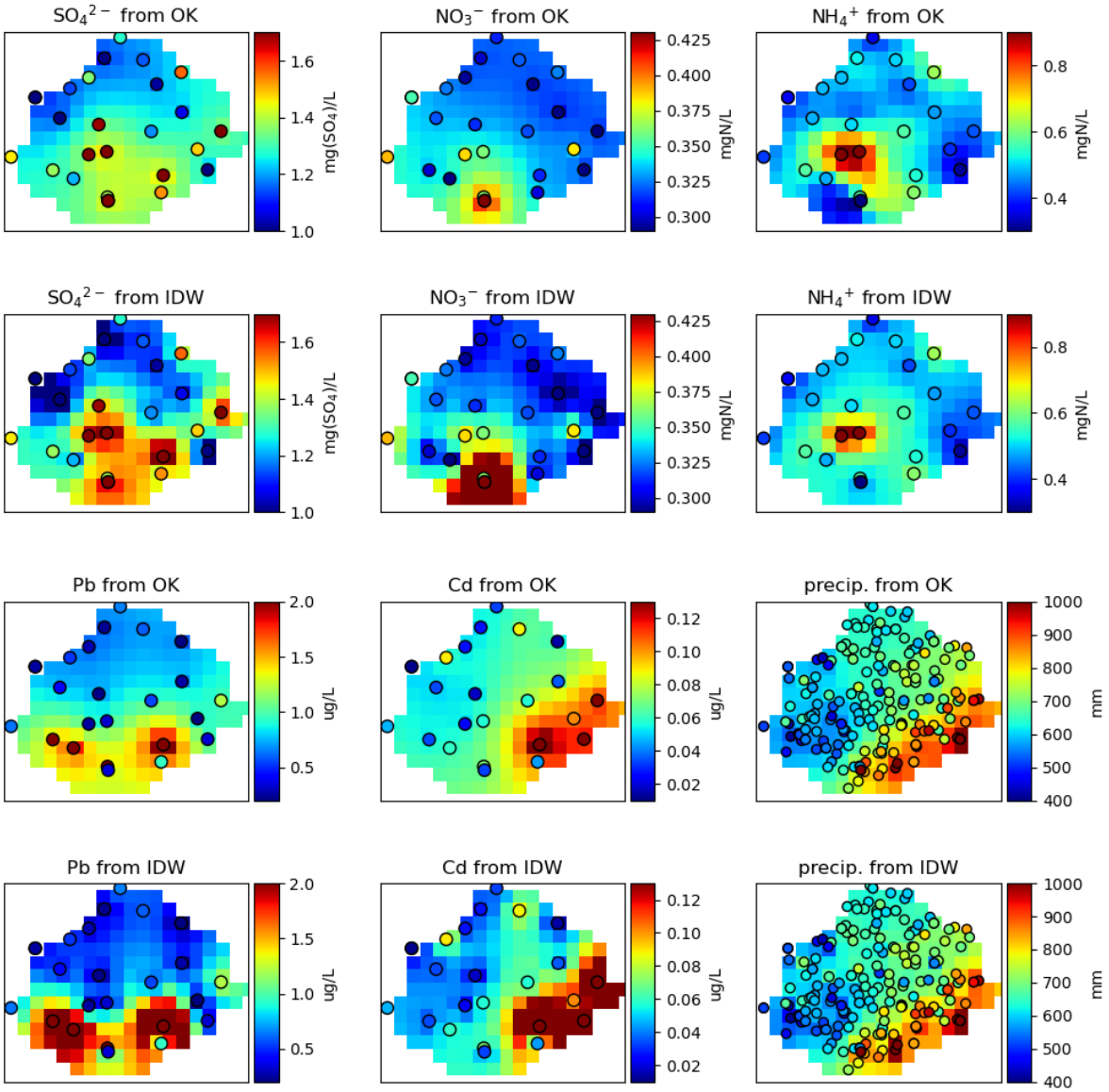

Figure 5: Comparing the spatial distribution of wet deposition in Poland using Ordinary Kriging (OK) that has been constrained with nugget=0 and Range = 4, and inverse distance weighting (IDW).

1.3 Calculate wet deposition from kriged results

To calculate wet deposition the concentrations are multiplied with the precipitation amount. The precipitation amounts are kriged at the same resolutions as the concentrations and wet deposition in 2020 is shown in Figure 6.

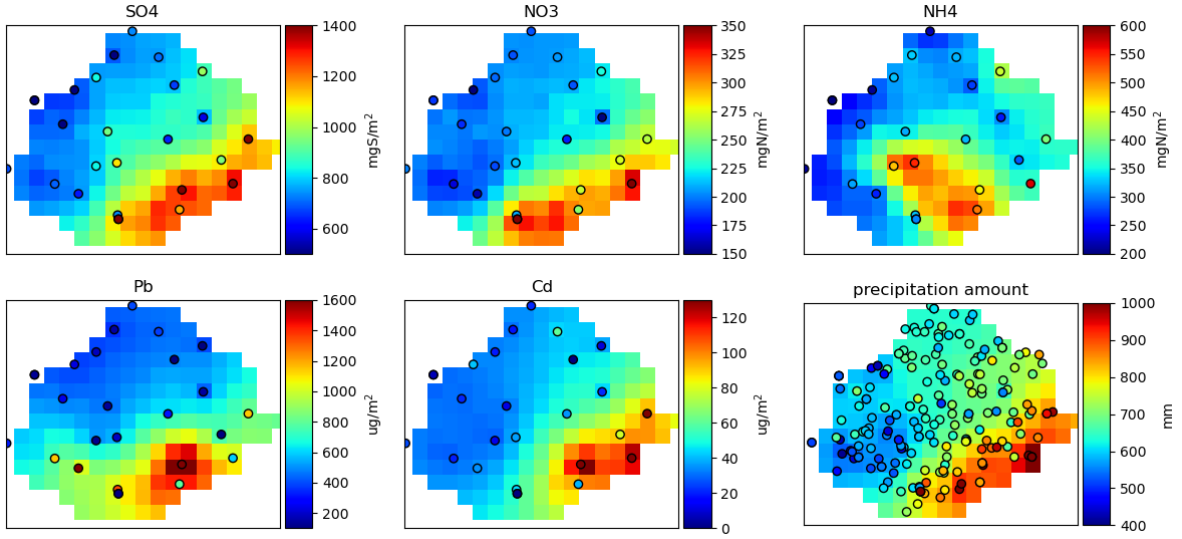

Figure 6: Wet deposition of various component in Poland in 2020 calculated using kriged concentrations multiplied with kriged precipitation amount in a 50x50 km grid (old EMEP grid). Observations used are superimposed.

To obtain higher resolution of the deposition one could use precipitation amount generated from other services instead of using the kriging on the observed annual precipitation amount. High resolution climatological dataset provided by either national or European meteorological services are available and tested more extensively than the simple kriging technique proved here. The Polish meteorological service IMGW-PIB provide data to the European Climate Assessment & Dataset project (https://www.ecad.eu) who make daily gridded observational dataset (E-OBS) of precipitation and other meteorological parameters, from 1950 to now. In Norway, the national product from the MET service with 1x1km gridded precipitation (https://github.com/metno/NWPdocs/wiki/MET-Nordic-dataset) is used to obtain high resolution wet deposition. This dataset using a combination of measured data from rain gauges, radars and models. These high-resolution observations can be combined with kriged data in coarser resolution to get fine scale deposition. This can be important especially in areas in undulant terrains where the precipitation amount may vary significantly over very short distances while the concentration gradient may be less varied.

An easy way of increasing the resolution is to krige the data into higher resolution. The polish data has been kriged into the EMEP 0.1x0.1° grid and wet deposition in same resolution has been calculated, Figure 7. This to enable easier comparison with the EMEP model, Figure 10. However, one should be careful in decreasing the grid size without having sufficient number of sites to provide that fine coarse information. In order to avoid these overly smooth results, for higher spatial resolution it might be useful to apply spatial auxiliary variables (e.g. using UK or regression kriging) that are to some extent correlated with the variable to be interpolated.

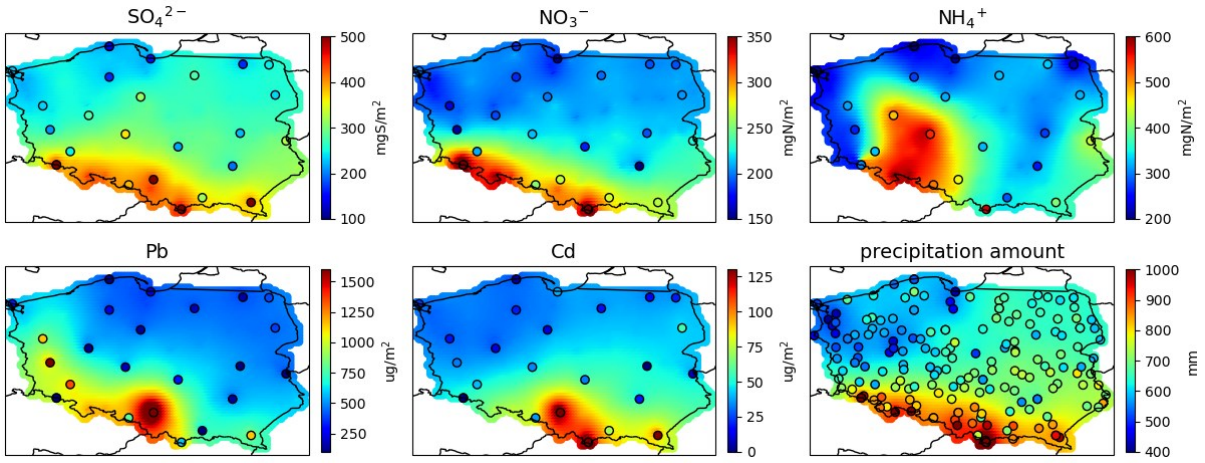

Figure 7: Wet deposition of various component in Poland in 2020 calculated using kriged concentrations multiplied with kriged precipitation amount in 0.1x0.1° EMEP grid. Observed depositions are superimposed.

1.4 Summary, points to note for statistical kriging

- For successful kriging it is important that the sites are representative, thus it is necessary with carefully assessment the representativity of the sites. When neighbouring sites show very different concentrations (before kriging), it may indicate that both are not representative for the area. This causes problems in the variogram models and predictions biased.

- It's important to have enough sites that reveal the spatial gradient in the area of interest. One way to increase the spatial coverage is to include data from neighbouring countries to improve the predictions in the border areas.

- Test different grid size for kriging. The grid size of the output maps needs to match the sampling density and scale at which the processes of interest occur. One can always try to produce maps by using the most detail grid size that our predictors allow us. Then, we can slowly test how the prediction accuracy changes grid sizes.

- Try out different constrains in defining the variogram models (i.e. nugget, range, sill and model). If the data show an anisotropy this should be considered added to the variogram model, including the angle of the principal direction (strongest correlation).

- Instead of applying kriging of the precipitation amount as shown in this report one should seek high resolution climatological dataset provided by either national or European meteorological services.

2 Observation-based mapping of European air quality using geostatistics (ETC/HE)

The European Topic Centre on human health and the Environment (ETC/HE) and its predecessors have been operationally generating annual observations-based concentration maps of air quality over Europe for many years. The method is based on geostatistical spatial interpolation of station observations with the help of various auxiliary variables. The advantage of a geostatistical approach over more simplistic spatial interpolation methods such as *inverse distance weighting* is that the former explicitly takes into account the spatial structure (autocorrelation) of the data and further provides an indication of the interpolation uncertainty. More specifically, the geostatistical method used within the ETC/HE is *residual kriging* (also known as *regression kriging*, *kriging with external drift*, or *universal kriging*) (Goovaerts, 1997; Chiles and Delfiner, 2009; Wackernagel, 2013). Compared to *ordinary kriging*, which often tends to produce unrealistically smooth maps for air quality applications, *residual kriging* allows for the exploitation of the spatial patterns available within the auxiliary datasets, and thus results in more realistic and detailed air quality maps.

Input data to the approach includes the station observations and various spatial auxiliary variables. The latter are typically:

- Output from the EMEP MSC-W model (Simpson et al., 2012).
- Meteorological parameters (surface solar radiation, temperature, wind speed, relative humidity, soil moisture) from the ERA5 reanalysis (Hersbach et al., 2020; Muñoz-Sabater et al., 2021).
- Elevation from GMTED2010 (Danielson and Gesch, 2011).
- Population density and -totals (Eurostat, 2014).
- Land cover from CLC2018[1].
- Road type vector data (Meijer et al., 2018).
- For the annual average of nitrogen dioxide (NO_2) satellite observations, the vertical column density of NO_2 from the TROPOspheric Monitoring Instrument (TROPOMI) onboard of the Sentinel-5P platform (Veefkind et al., 2012; Van Geffen et al., 2020).

The method uses a linear regression model between the station observations and the predictor variables with subsequent kriging of the residuals, where the variogram is estimated using a spherical function. As the spatial autocorrelation of the station observations varies significantly between urban and rural stations, interpolation is carried out separately for rural and urban areas and the results are subsequently combined into the final map. More details of the approach used in the ETC/HE can be found in Horálek et al. (2021).

The maps produced as part of the ETC/HE have been used for various applications including the annual "Air quality in Europe report" published by the European Environment Agency (EEA, 2020). Figure 8 shows an example of the 2019 annual average of $PM_{2.5}$.

[1] https://land.copernicus.eu/pan-european/corine-land-cover/clc2018

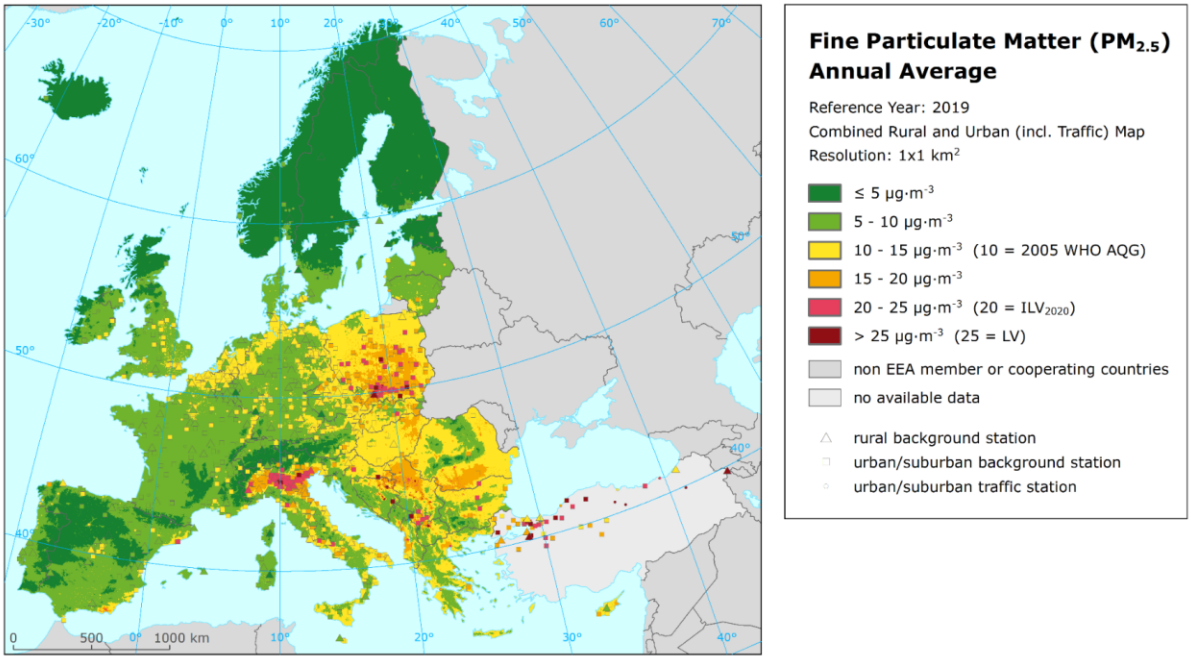

Figure 8: Example of a spatially interpolated European annual average air quality map of fine particulate matter for the year 2019 produced within the ETC/HE. The coloured symbols show the location and measured value of all air quality monitoring stations used in the mapping. From Horálek et al. (2021).

3 Modelling deposition of particulate matter, acidifying and eutrophying components, metals and POPs

Atmospheric pollution has profound effects on ecosystems, climate, and human health, and high concentrations and deposition of nitrogen and sulfur can be a challenge. One of the ways high levels of pollutants can impact ecosystems and soil nutrient levels is via the process of wet deposition. Wet deposition involves the removal of polluting trace gases when they dissolve in cloud or rain droplets and are then removed by precipitation. Though to a lesser degree, the ecosystems can also be impacted by dry deposition. Dry deposition is the process of pollutants impacting the ground, a plant, or another surface and subsequently being removed from the atmosphere. Because it is dry, this process is entirely driven by winds and gravity, not rainfall or fogs. Atmospheric chemistry and transport models (CTMs) are important tools to understand sources and impacts of nitrogen and sulfur chemistry and potential mitigation and to further our knowledge of wet deposition. Such models offer complementary information to observation-based methods alone by offering continuous spatio-temporal coverage. Their limitation is that we may expect the information from models to be less accurate than observation-based methods, especially estimates close to the sites, depending on the robustness in the emission estimates and the model scheme.

3.1 Modelling deposition of particulate matter, acidifying and eutrophying components

For studies of air pollution and deposition in Europe, the EMEP MSC-W (European Monitoring and Evaluation Programme Meteorological Synthesizing Centre - West) chemistry transport model is a useful tool. The model has been developed by MET Norway (Simpson et al., 2012; https://www.emep.int) and is an open-source Eulerian grid model used for applications ranging from scientific research to policy development (e.g. Bergström et al., 2014; Karl et al., 2019; Jonson et al., 2017; McFiggans et al., 2019, Ge et al., 2021). The standard model uses 21 terrain-following vertical layers, with the pressure ranging from around 1000 hPa (surface level) to 100 hPa (highest level). Output surface concentrations for major species are adjusted to be equivalent to 3 m above the surface as described in Simpson et al. (2012). Parameterisation of the wet deposition processes in the EMEP model includes both in-cloud and below-cloud scavenging of gases and particles.

The EMEP model is often run with gridded anthropogenic emissions from CEIP (EMEP Centre on Emission Inventories and Projections) which are categorized into 11 SNAP sectors. The emissions are also conducted and prepared for modelling using the 13-sector GNFR system or 19-sector GNFR_CAMS system (after 2020). However, the model can also be run with any other gridded emission files as long the abovementioned SNAP or GNFR sectors are used.

The standard meteorological drivers for the EMEP model are from the Integrated Forecast System model (IFS) of the European Centre for Medium-Range Weather Forecasts (ECMWF), named ECMWF-IFS (Fagerli et al., 2019; Pommier et al., 2020). These data have a resolution of 0.1° x 0.1° degree and cover the entire Europe and the eastern EECCA countries. However, the EMEP model is relatively flexible when it comes to meteorology and can be run with other drivers than ECMWF-IFS.

Every year a comprehensive EMEP report is published, which presents transboundary fluxes of particulate matter, photo-oxidants, acidifying and eutrophying components. Figure 9 is taken from the last report (Fagerli et al., 2022) and shows total wet deposition of reduced nitrogen (ammonia and ammonium) in 2020, where modelled values are compared to measurements at EMEP sites. For reduced nitrogen, the annual average over all EMEP sites is 0.62 mgN/m^2·day, whereas the modelled average is 0.67 mgN/m^2·day (Appendix D in Fagerli et al., 2022). The spatial correlation between measurements and model is 0.64. For wet deposition of oxidized nitrogen, the spatial correlation between observations and model is somewhat higher, i.e. 0.75.

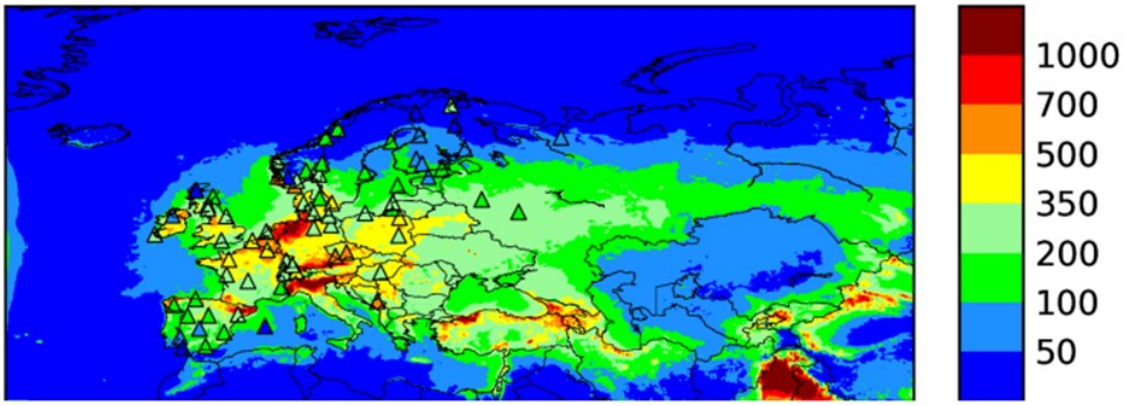

Figure 9: Modelled wet deposition of reduced nitrogen (mgN/m^2) in 2020, with EMEP observations on top (triangles). From Figure 2.14 in Fagerli et al. (2022).

The EMEP model has gradually become more user friendly, where preferred parameters and output options are specified in ascii input files. The map projection and resolution of model output are automatically adjusted to match the meteorological input files. The users often need flexibility regarding map projection and resolution, model domain and time period, thus, the last years it has become more common to run the EMEP model with WRF meteorology.

WRF - Weather Research and Forecast model (http://www.wrf-model.org; Skamarock et al., 2008) is a mesoscale numerical weather prediction system designed to serve both operational forecasting and atmospheric research needs. WRF is freely available and has a large number of users all over the world. It is designed to be a flexible, state-of-the-art atmospheric simulation system suitable for use in a broad range of applications across scales ranging from meters to thousands of kilometres.

The combination of WRF and EMEP (WRF-EMEP) is frequently used in Norway to study the impact of strong emission sources (e.g., industry) and deposition close to the sources. For such inventories, a spatial grid resolution of 1km is typically used. WRF-EMEP has also been applied in other parts of the world, for example as the core models of an air pollution forecasting system in the Hubei province in China, and in projects linked to offshore oil and gas industry (e.g., Karl et al., 2015).

The modelled results available from https://www.emep.int/mscw/mscw_moddata.html with consistent timeseries from 1990 to 2020. I.e., the same data as presented in Figure 9 can be prepared from the NetCDF files available, and in Figure 10 these are compared with all the Polish data from 2020.

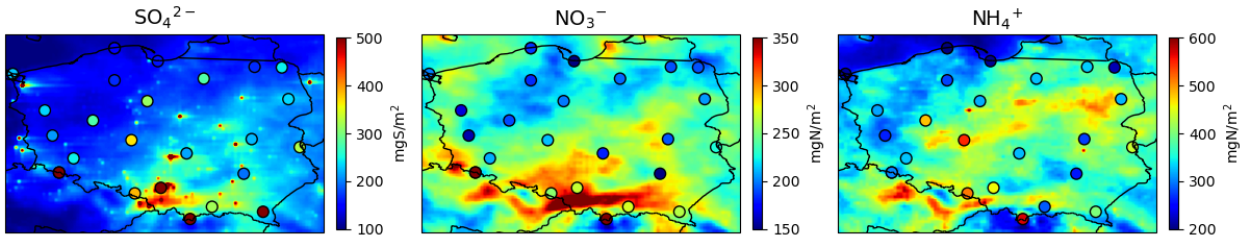

Figure 10: Wet deposition of sulfate, nitrate and ammonium in Poland in 2020 calculated by the EMEP model, with observations superimposed.

There are also other models that can be used for assessing deposition of nitrogen and sulfur. Poland uses the chemical transport model GEM-AQ (Global Environmental Multiscale model- Air Quality, Kaminski et al., 2008), as presented in Chapter 3.2.2.

3.1.1 Dry deposition of trace gases

This section describes some of the theory related to the process of dry deposition and is designed to give a summary of the current state of the art on the study of this process. It is the intention that this information could be used to formulate the required specifications for a call to tender aimed at developing a dry deposition service at the national level in Poland. Furthermore, it is necessary to describe dry deposition separately from wet deposition because the same means for observing wet deposition of pollutants cannot be applied in the case of observing dry deposition of pollutants in the environment. Indeed, the measurement of dry deposition is extremely complex and it can only be measured indirectly. As a result, observations of dry deposition are not used to study the environmental impacts of this process and modelling represents the current state-of-the-art for its study.

Dry deposition involves the removal from the atmosphere of trace gas pollutants via their interaction with the land surface. This interaction can take different forms, i.e., dissolution into surface water, chemical reaction with organic matter, and even adsorption, which is a chemical term for when gases stick to solids. Due to these different processes, the different properties of pollutants, and the varied nature of the land surface, simulating dry deposition is a complex task.

Chemical transport models use parameterisations in order to simulate dry deposition and to try to reduce some of this complexity of representing this process across many surface types for different gases, while still providing a plausible physical model. The parameterisations currently in use are based on an electrical current resistance-analogy model (Wesely, 1989; Zhang et al., 2003) whereby resistances in series and in parallel represent simultaneously the competing deposition of gases via different processes. Figure 11 represents the most commonly resistance types and how they link together in series and in parallel.

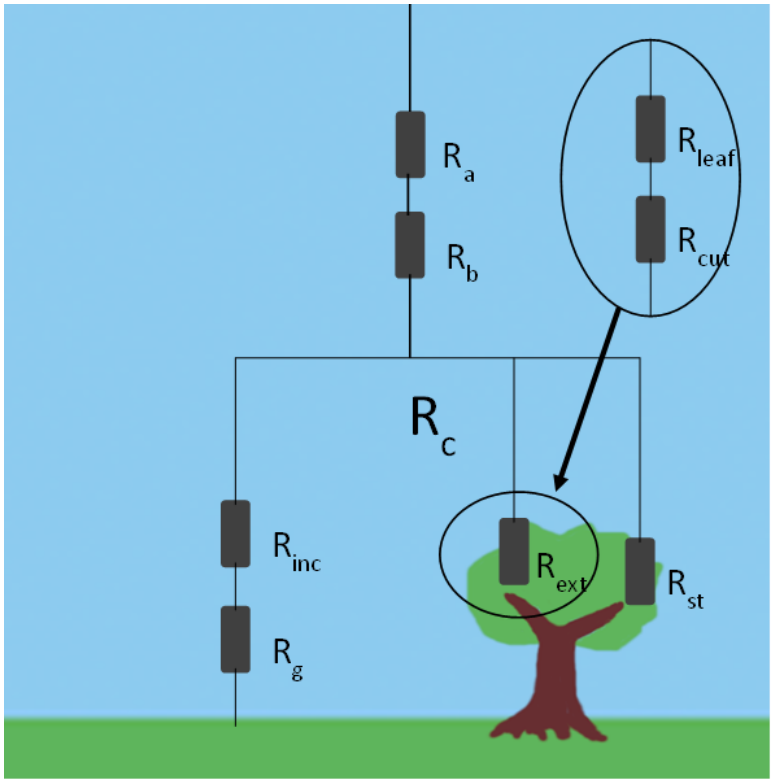

Figure 11: Schematic diagram showing the different kinds of resistance used in parameterisations of dry deposition. The three main resistances, R_a (aerodynamic resistance), R_b (quasi-laminar layer resistance), and R_c (canopy resistance) are arranged in series. There are then three systems of resistance arranged in parallel, R_{st} (stomatal resistance), R_{inc} (in-canopy resistance) and Rg (ground resistance) in series together, and Rext (external leaf resistance). Rext consists of Rleaf (leaf resistance, and Rcut (cuticular resistance) in series with one another.

The three main resistance types (aerodynamic, quasi-laminar layer, and canopy resistance) combine together in series by taking the reciprocal of their sum,

$$V_d = \frac{1}{R_a + R_b + R_c}$$

which yields a quantity termed deposition velocity, V_d. Deposition velocity can then be used to calculate the pollutant concentration flux to the surface, *F*, by multiplying it with the pollutant concentration, *C*.

$$F = C \times V_d$$

Dry deposition velocities are therefore the parameter that mediates the deposition of pollutants to the surface within this conceptual model. The simulation in models of the various types of resistance that control deposition velocity are linked to different meteorological variables and land surface properties. For example, aerodynamic resistance is a measure of much the level of turbulence in air over the surface, which is linked to wind speed, vertical stability, and surface roughness (a measure of the height and spacing of surface obstructions like vegetation and buildings). Aerodynamic resistance is therefore highly dependent on having good meteorological data including good spatial and temporal coverage.

In another example, the canopy resistance is highly dependent on vegetation characteristics such as plant functional type (i.e., forest type, crops, shrubs, etc.), the amount of foliage quantified by leaf area index, and photosynthetic activity. Photosynthetic activity is important because it affects whether plant stomata are open or closed, and stomata represent an important deposition mechanism for gases. Modelling the deposition over vegetation therefore requires detailed knowledge of land use and vegetation mapping as well as data or a model of plant photosynthetic activity during the diurnal cycle.

Dry deposition velocities can vary greatly in space due the different processes described above. Figure 12 gives an example of the of the spatial variability one can expect for SO_2, NO_2, and NH_3 dry deposition velocity over Poland. In addition to the spatial heterogeneity of these data, there are also significant uncertainties for estimating dry deposition velocities due to uncertainties in land surface properties and uncertainties in the dry deposition resistance model parameters. Figure 13 shows the dry deposition velocities estimated by a vegetation model that is based on satellite observations of leaf area index, and Figure 14 shows the absolute differences resulting from using these two different vegetation schemes. Similarly, Figure 15 shows the kind of differences we can expect from different simulations based on a different dry deposition scheme. Various different schemes exist based on the resistance-analogy method, e.g., the original Wesely (1989) scheme that is still widely used, a more recent yet still widely used scheme, Zhang et al. (2003), and the scheme implemented within the EMEP chemical transport model, Simpson et al. (2012).

In addition to the dry deposition of gases, it is important to add dry deposition of aerosol to the total budget of dry deposition. Dry deposition of aerosols is driven by turbulence and shows a strong dependence on particle size. The smaller the particles the smaller the deposition rate. Thus, fine aerosols have a longer lifetime and have potential to be transported several hundred kilometres before deposited, depending on weather and surface conditions.

Figure 16 shows the spatial variability in total dry deposition of SO_x, NO_x, and NH_x over Poland in 2020 simulated by the EMEP model.

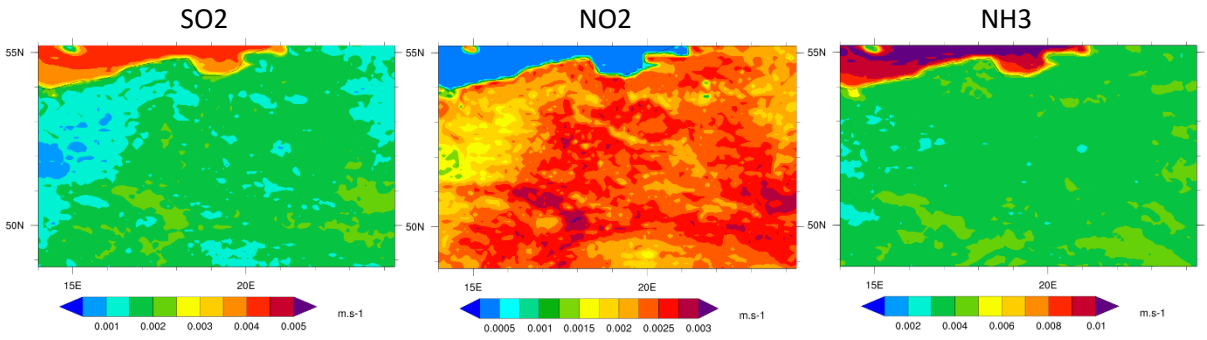

Figure 12: Dry deposition velocities for SO_2, NO_2, and NH_3 over Poland for 2020 as calculated by the SURFEX land surface model (using the EMEP dry deposition scheme). The land surface model was run with a standard vegetation simulation scheme. Units: $m.s^{-1}$.

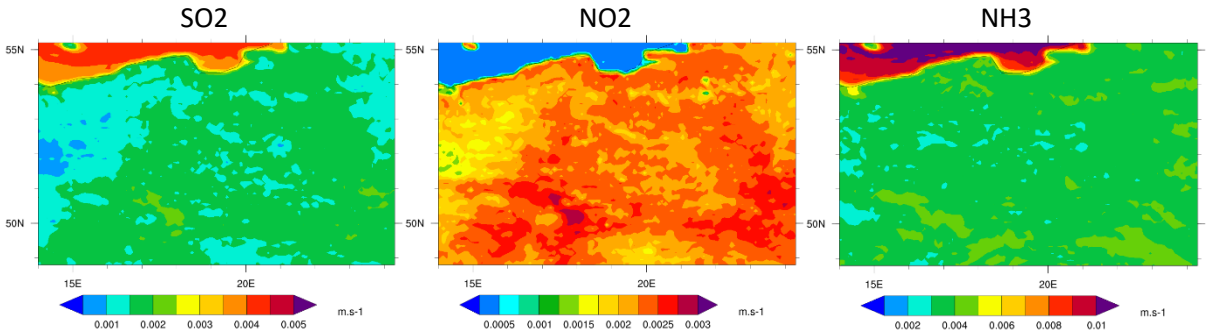

Figure 13: Dry deposition velocities for SO_2, NO_2, and NH_3 over Poland for 2020 as calculated by the SURFEX land surface model (using the EMEP-based dry deposition scheme). The land surface model was run with vegetation derived from satellite observations of leaf area index. Units: $m.s^{-1}$.

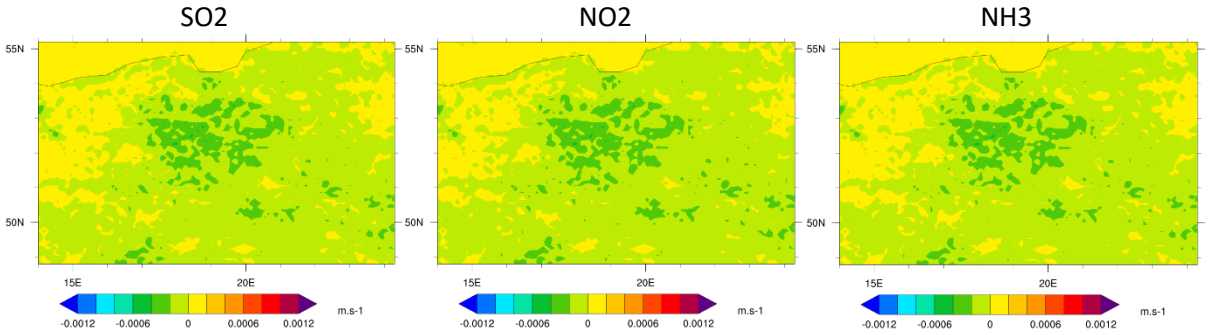

Figure 14: The difference in simulated dry deposition velocities for SO_2, NO_2, and NH_3 over Poland for 2020 between a simulations where the land surface model was run in a standard configuration and where the land surface model was run with vegetation derived from satellite observations of leaf area index. The results show the satellite-derived vegetation minus standard simulation difference. Units: $m.s^{-1}$.

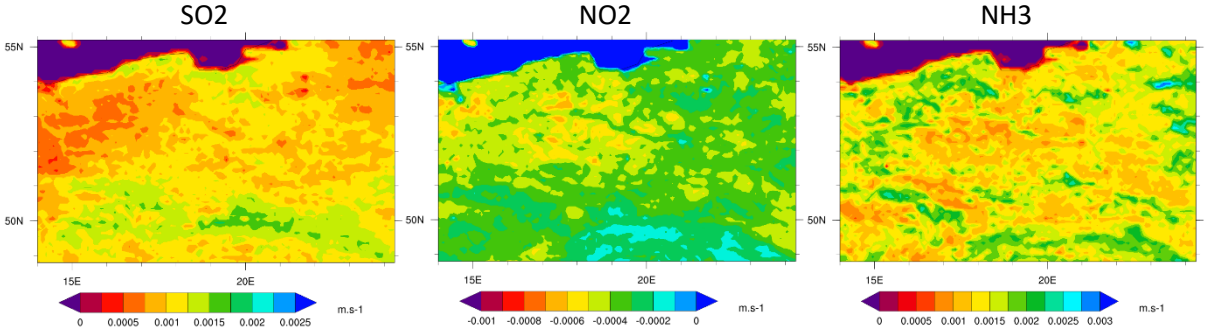

Figure 15: The difference in simulated dry deposition velocities for SO_2, NO_2, and NH_3 over Poland for 2020 between results from the SURFEX land surface model run using the EMEP-based dry deposition and Wesely (1989) dry deposition schemes. The results show the EMEP minus Wesely dry deposition data. Units: $m.s^{-1}$.

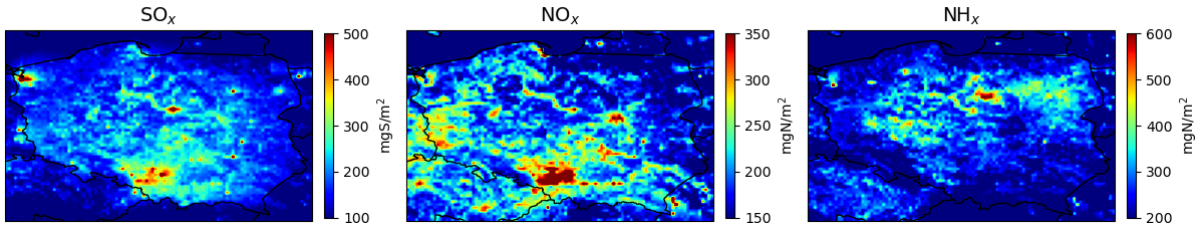

Figure 16: Total dry deposition of sulfur, oxidized- and reduced nitrogen in Poland in 2020 calculated by the EMEP model. Units: mg.m^{-2}.

One important point to raise is the contrast between the spatial variability of dry deposition velocity (as shown in Figure 12 and Figure 13) and dry deposition flux (as shown in Figure 16). The difference in spatial patterns arises from the fact that deposition flux relies on the concentration of the pollutant, Thus, a suitable model for simulating atmospheric concentrations of pollutants must be used in conjunction with a model of dry deposition in order to derive fluxes.

Neither deposition fluxes nor deposition velocities are operationally monitored. Instead, only isolated observations over specific land use types exist which have been used to help to validate the approach. Modelling of dry deposition therefore remains the only method in existence to estimate dry deposition processes over large spatial scales and for continuous periods of time.

Points to note:

- Deposition modelling using a resistance analogy model provides a suitable means of estimating dry deposition for reactive gases over large spatial scales, different surface and for continuous periods of time.
- Differences in representation of vegetation and in deposition scheme can introduce uncertainties into estimates of dry deposition processes.
- Adequate care should be taken to ensure sufficient quality of underlying deposition model, land use and vegetation input data should be of high quality, and meteorological parameters should be taken from a reliable source.
- The dry deposition velocities need to be coupled with a model of atmospheric pollution of sufficient quality in order to guarantee good quality estimates of dry deposition pollutant fluxes.

3.2 Modelling heavy metals and POPs

POPs are a group of toxic, persistent, and semi volatile chemicals capable to be accumulated in environmental compartments and in biological chains. Likewise, heavy metals bio-accumulate and are toxic to biota. A unique feature of POPs and mercury is their ability for re-emission. To evaluate the long-range transport and deposition of these pollutants, a multi-compartment modelling approach is required. The exchange with and accumulation in the main environmental compartments (atmosphere, soil, seawater, and vegetation) is described by basic processes: emission, long-range transport, deposition, degradation, and gaseous exchange between the atmosphere and the underlying surface.

3.2.1 GLEMOS modelling framework (EMEP MSC-East)

The global modelling framework GLEMOS is a multi-scale multi-pollutant simulation platform developed for operational and research applications within the EMEP programme [Travnikov and Jonson, 2011]. The framework allows simulations of dispersion and cycling of heavy metals and persistent organic pollutants in the environment with a flexible choice of the simulation domain (from global to local scale) and spatial resolution. The modular architecture of the modelling system allows flexible configuration of the model set-up for a specific research task and pollutant properties. Currently, the modelling system includes three major groups of substances: mercury, particle-bound heavy metals (Pb, Cd) and POPs.

GLEMOS allows application on different geographical scales with various spatial resolutions. The base model grid on a global scale has horizontal resolution 1°×1°, and the standard regional model domain covers the EMEP region (30°N-82°N, 30°W-90°E) with a spatial grid that has a changeable resolution down to 0.1°×0.1°. In addition, a variety of smaller domains can be used for national scale case studies. Vertically, the model domain covers a height up to 10 hPa (ca. 30 km). The current vertical structure consists of 20 irregular terrain-following sigma layers, with the first 10 layers covering the lowest 5 km of the troposphere and the height of the lowest layer is about 75 m.

GLEMOS includes parameterizations describing atmospheric, ocean, soil, and media exchange processes. More detailed descriptions of the model parameterisations and approaches is available in a series of technical reports (Travnikov and Ilyin, 2005; Gusev et al., 2005; Tarrason and Gusev, 2008; Travnikov et al., 2009; Jonson and Travnikov, 2010; Travnikov and Jonson, 2011; EMEP MSC-E Report 2021).

The emission datasets for model assessment of HMs and POPs long-range transport within the EMEP region are prepared by Centre of Emission Inventories and Projections (CEIP) on the basis of officially submitted data (http://www.ceip.at/, latest available: 2019). The estimates of wind re-suspension of particle-bound heavy metals (Pb, Cd) and gaseous re-emission of Hg are based on the model parameterization that is still under development (Travnikov and Ilyin, 2005; Gusev et al., 2006; Gusev et al., 2007).

Like EMEP model for assessing particulate matter, photo-oxidants, acidifying and eutrophying components (Simpson et al 2018), the meteorological input information is typically generated from the operational analysis data of the ECMWF using the meteorological preprocessor based on the WRF. Land cover data were obtained from the International Geosphere-Biosphere Programme (IGBP) data layer of the Terra and Aqua combined Moderate Resolution Imaging Spectroradiometer (MODIS, Land Cover data product MCD12Q1, version 6, Friedl et al., 2019).

GLEMOS was extensively evaluated in several numerical experiments and multi-model studies within the Task Force on Hemispheric Transport of Air Pollution (TF HTAP) and multi-model assessments within the Global Mercury Observation System (GMOS) project (Travnikov et al., 2017) and the Global Mercury Assessment 2018 (AMAP/UN Environment, 2019).

EMEP MSC-E Report (2021, 2022) serves as supporting material if the reader is interested in the latest assessments done by the MSC-E on heavy metals and POPs (including what datasets were used as input and how the model was set up. The modelled total depositions are available at https://www.msceast.org/pollution-assessment/emep-domain-menu/data-hm-pop-menu For wet and dry deposition specifically, MSC-E provide this data off line. Figure 17 shows the comparison between modelled wet deposition of Cd and Pb and Polish observations in 2020 in

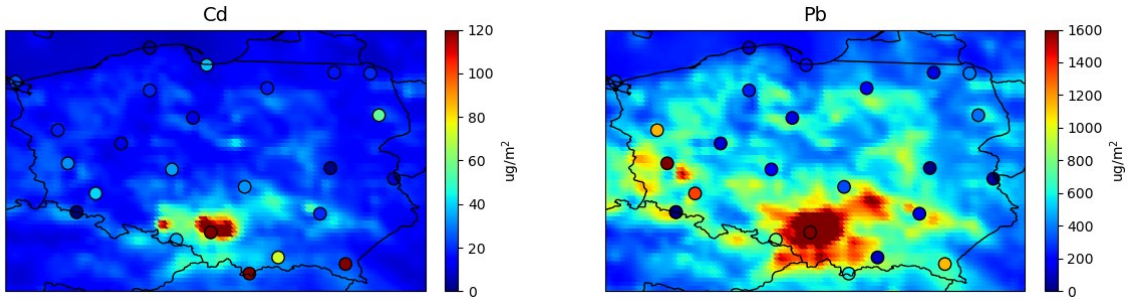

Figure 17: Wet deposition of cadmium and lead in Poland in 2020 calculated by the EMEP models with observations superimposed.

An assessment of cadmium atmospheric pollution levels in Poland in 2014 in presented in Ilyin et al (2018). This study includes an analysis of national emission and monitoring data, model-based source apportionment in particular Polish voivodships and pollution in the selected cities.

3.2.2 Other models available

Multimedia compartment models have been used to evaluate environmental fate on different scales. The following models are just some examples of models available that include atmospheric, soil and ocean modules and a parameterization describing the exchange processes between air and surface compartments.

- DEHM-POP was developed to study the atmospheric transport and environmental fate of POPs (Hansen et al., 2004). It is based on the Danish Eulerian Hemispheric Model (DEHM, Christensen, 1997), a 3-D Eulerian dynamical atmospheric. DEHM has also been expanded to study the atmospheric transport of lead (Christensen, 1999).
- NEM (nested multimedia fate and transport model for organic contaminants, Beivik et al., 2021) builds on two existing multimedia fate and transport models (MFTMs) builds upon CoZMo-POP2 (Wania et al., 2006) and BETR-GlobalM (Macleod et al., 2011), two models for predicting the long-term behaviour of POPs in the physical environment. NEM adopts major parts of the code from CoZMo-POP2 and supplements it with parts of the parameterization of BETR-Global. A key feature of NEM is the opportunity to operate the model across different spatial scales and resolutions to focus on a specific region of the globe, offering increasing resolution with increasing proximity to a given target region of interest.
- MPI-MCTM (Max Planck Institute multicompartment chemistry–transport model, Lammel et al., 2001) based on a general circulation model of the atmosphere, ECHAM4 (Roeckner et al., 1996).
- GEOS-Chem is a global 3-D model of atmospheric chemistry driven by meteorological input from the Goddard Earth Observing System (GEOS) that was extended to simulate PAHs to improve POPs modelling (Friedman and Selin, 2012).

3.3 Modelling capabilities in Poland

GEM-AQ (Global Environmental Multiscale model- Air Quality, Kaminski et al., 2008) is a modelling system for tropospheric chemistry and air quality that has been used by the Warsaw University of Technology since 2003. This modelling system was intended to be used by air quality management authorities operationally (Struzewska and Kamiski, 2010). A high-resolution nested forecast at 5 km resolution over Poland (and surrounding countries) was implemented in December 2012 (EcoForecast.EU, Kaminski and Struzewska, 2013) and, since 2015, there is a cooperation with the Copernicus Atmosphere Monitoring Service (CAMS, Marécal et al., 2015). CAMS is based on state-of-the-art numerical air quality models developed in Europe and each of the eleven partners provide regional daily forecasts of the main atmospheric pollutant concentrations on a 10 to 20 km horizontal resolution. The models also perform daily retrospective analyses of pollutants near the surface by assimilating 1-day old observations from the Near-real-time (NRT) service for air quality measurements over Europe from the European Environmental Agency (EEA). In addition, the models are constantly verified against European surface station observations for O_3, NO_2, SO_2, CO and PM_{10} and $PM_{2.5}$ through maps and statistical indicators. Currently it is the Institute of Environmental Protection – National Research Institute (IEP-NRI) that is providing the regional air quality data.

GEM-AQ integrates the Global Environmental Multiscale model (GEM) (Côté et al., 1998a), developed at the Canadian Meteorological Centre and used for operational weather prediction, with air quality chemistry, including the gas phase, aerosol and cloud particles, wet chemistry, emission, deposition and transport processes. GEM-AQ has also been augmented to study POPs (Kamiski et al. 2020, Gong et al., 2007; Huang et al., 2007). The GEM-AQ model has been run in several configurations ranging from a global (O'Neill et al., 2006) and regional domain (Kaminski et al., 2008) to high resolution studies (Struzewska and Kaminski, 2008) and showed good agreement with observations of aerosol optical properties, gaseous species concentrations, and seasonal variation of POPs in the atmosphere.

4 Measurement model fusion (MMF)

The overall concept of MMF involves bias correcting CTM using observational data to create fused deposition maps (Fu bet al 2022). National MMF products have been developed in U.S (Schwede et al., 2014), Canada (Schwede et al., 2019), and Sweden (Andersson et al., 2018). Other national products are under developments like in Norway (Aas et al., 2017). The World Meteorological Organization's Global Atmosphere Watch Programme (WMO GAW) has initiated a project specifically focused on improving the tools for MMF products with the aim of providing maps of Global Total Atmospheric Deposition (GTAD). The MMF GTAD project is presented by Fu et al. (2022) and here they present conceptual methodology as described in Figure 18.

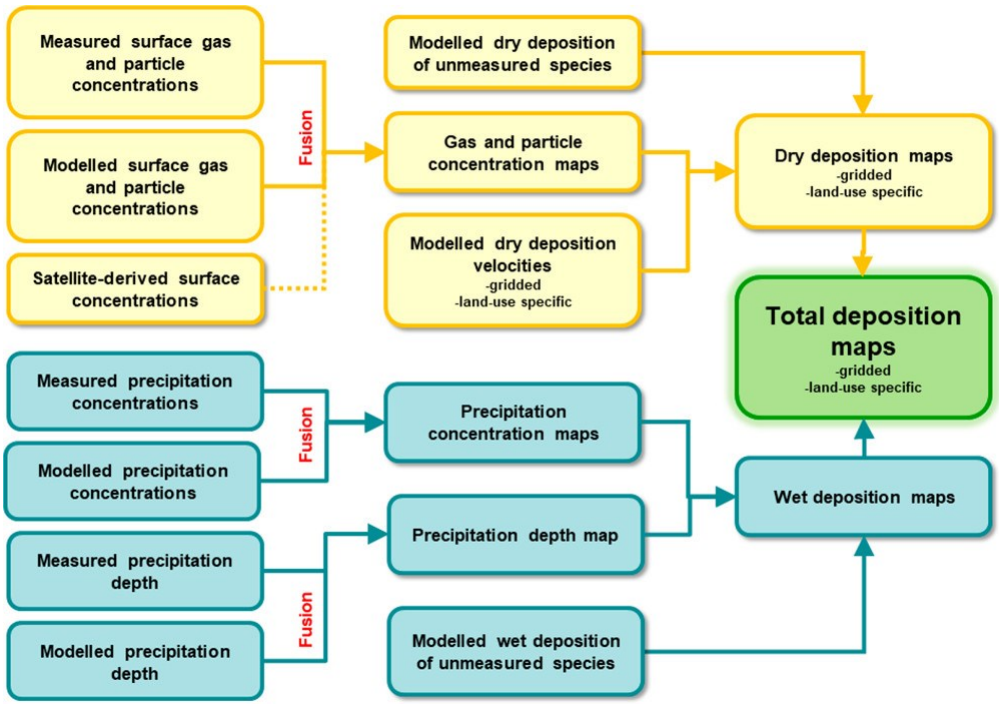

Figure 18: A general methodology for producing global total deposition maps as presented by Fu et al. (2022).

In this example, for both wet and dry deposition, the concentrations from the model and the observations are fused to create maps of concentrations before calculating the deposition. It is better to do the fusion on concentrations in air and precipitation rather than deposition, since the former has a smoother spatial variation which is beneficial for the method. A higher resolution can be achieved in the final deposition fields by combining the data analysed concentration fields with high resolution boundary layer meteorology and precipitation, meaning if the precipitation dept map has higher resolution than the concentration maps.

How the fusion between observations and models are done is defined by Fu et al. (2022), different methods are used. I.e.:

- In Sweden, Andersson et al (2018) perform a variational data (2dvar) analysis using the MATCH model fused with observations from national networks and neighbouring countries.
- In US, the total deposition (TDEP) products have been developed over many years and is working operational (https://nadp.slh.wisc.edu/committees/tdep/). Schwede et al presented

their method in 2014: “The measured data were interpolated into grids using inverse-distance weighting (IDW). The maximum distance of influence used in the IDW were determined from examining the spatial correlation in the CMAQ gridded average seasonal concentration data using a variogram analysis. For each chemical and season, they plotted the sample variogram and then fitted an exponential covariance model with three parameters (nugget, sill, and range) using a nonlinear least squares algorithm. The covariance model was then normalized and plotted against distance. Distances corresponding to a covariance of 0.7 were determined for each chemical species for each season and used in the IDW”.

- In Canada, the ADAGIO model Canada (Atmospheric Deposition Analysis Generated from optimal Interpolation from Observations described by Schwede et al, 2019. Measured concentrations used to adjust modelled concentrations from ECCC’s GEM–MACH (Global Environmental Multiscale–Modelling Air quality and Chemistry) model using optimal interpolation techniques which minimizing the differences between the model and measurements.
- In Norway the deposition of nitrogen and sulfur for the period 2012-2016 combining observations and EMEP model described by Aas et al, (2017).: “For all measurement points, the difference between the measured value at that point and the modelled value in the corresponding grid cell is calculated. This difference is interpolated spatially using radial basis functions, giving a continuous two-dimensional function describing the difference at any point within the modelled grid. The combined maps are derived adjusting the model results with the interpolated differences, giving large weight to the observed values close to stations, and using the modelled values in areas with no observations. The range of influence of the measured values has been set to 500 km for all the species”.

The CTM model provides dry deposition velocities. Depending on the CTM used, deposition velocities may be available as grid averaged or land-cover specific values. These dry deposition velocities are combined with the fused air concentration field to calculate the total dry deposition Figure 18. Total deposition is found by combining wet and dry deposition.

5 General remarks and recommendations

A general recommendation is that both models and observations should be used when assessing the atmospheric deposition. Combining observations and modelling improves the modelled estimates by reducing model biases and provides a more sophisticated method for describing the variation between measurement sites than merely using interpolation methods of measurements such as kriging.

For wet deposition, there are usually more observations and interpolation can give reliable spatial information. It is important to use precipitation amount from the denser meteorological network comparted to the network for chemical composition. One should seek high resolution climatological dataset provided by either national or European meteorological services.

For dry deposition one should either use only model results or combining measurement-model, i.e., dry deposition velocities should be taken from models.

One should test different methods and approaches, assess the differences to better understand which method or combination of methods is best in each case. It might be different depending on different components and the availability of data and model results. One should check if the methods are sensitive to differences between seasons. Table 1 gives an overview of which methods are available and recommended to use for the different components. When using the results from atmospheric transport models it is important to use observations for validation.

Table 1: Overview of the different approaches recommended for estimating atmospheric deposition.

Component	Observations, spatial interpolation methods	Chemical transport modelling	Measurement model fusion
SO_4, NO_3, NH_4 wet deposition	X (if sufficient number of observations combined with dense national network on precipitation amount)	X	X
SO_4, NO_3, NH_4 dry deposition	Not recommended (possible to apply kriging on concentrations combined with dry deposition velocities from literature or model)	X	X
Cd, Pb + other trace elements wet deposition	X (if sufficient number of observations and combined with national network on precipitation amount)	X	maybe
Cd, Pb + other trace elements dry deposition	Not recommended	X	maybe
Hg wet and dry deposition	Not recommended (too few sites and bidirectional fluxes)	X	-
-POPs wet and dry deposition	Not recommended (too few sites and bidirectional fluxes)	X	-

When using observations, it is important to carefully assess whether they are representative for a larger area and of sufficient quality. To do this one need to involve people who knows the data and have experience in data handling and evaluation of the quality and representativity in the observations used. For the statistical method it is necessary to have some statistical knowledge. It is easy to get wrong results just applying an interpolation technique. It is also recommended to include experts in chemical transport modelling in the assessment of atmospheric deposition.

6 References

Aas, W., Hjellbrekke, A-G., Fagerli, H. and Benedictow, A. (2017). Deposition of major inorganic compounds in Norway 2012–2016. NILU OR 41/2021. Kjeller, NILU, http://hdl.handle.net/11250/2485535.

AMAP/UN Environment (2019). Technical Background Report for the Global Mercury Assessment 2018. Arctic Monitoring and Assessment Programme, Oslo, Norway/UN Environment Programme, Chemicals and Health Branch, Geneva, Switzerland. viii + 426 pp including E-Annexes.

Andersson, C.; Wylde, H. A.; Engardt, M. (2018). Long-Term Sulfur and Nitrogen Deposition in Sweden 1983-2013. SMHI METEOROLOGY No. 163.

Bergström, R., Hallquist, M., Simpson, D., Wildt, J., and Mentel, T. F. (2014). Biotic stress: a significant contributor to organic aerosol in Europe?, Atmos. Chem. Phys., 14, 13643–13660, https://doi.org/10.5194/acp-14-13643-2014.

Breivik, K., Eckhardt, S., McLachlan, M.S., and Wania, F. (2021). Introducing a nested multimedia fate and transport model for organic contaminants (NEM), Environ. Sci.: Processes Impacts, 23, 1146–1157

Chiles, J.-P., & Delfiner, P. (2009). Geostatistics: Modeling spatial uncertainty (Vol. 497). John Wiley & Sons.

Christensen, J. H. (1997). The Danish Eulerian Hemispheric Model – a three-dimensional air pollution model used for the Arctic, Atmos. Env., 31, 4169–4191.

Christensen, J. H. (1999). An overview of Modelling the Arctic mass budget of metals and sulphur: Emphasis on source apportionment of atmospheric burden and deposition, In: Modelling and sources: A workshop on Techniques and associated uncertainties in quantifying the origin and long-range transport of contaminants to the Arctic, Report and extended abstracts of the workshop, Bergen, 14–16 June 1999, AMAP report 99:4 (http://www.amap.no/).

Côté, J., Gravel, S., M ́ethot, A., Patoine, A., Roch, M., and Staniforth, A. (1998). The operational CMC–MRB Global Environmental Multiscale (GEM) Model. Part I: Design considerations and formulation, Mon. Wea. Rev., 126, 1373–1395.

Danielson, J. J. and Gesch, D. B. (2011). Global multi-resolution terrain elevation data 2010 (GMTED2010), U.S. Geological Survey Open-File Report, pp. 2011-1073 (https://pubs.er.usgs.gov/publication/ofr20111073) accessed 29 November 2022.

EEA (2020). Air quality in Europe: 2020 report. European Environment Agency. Publications Office. https://data.europa.eu/doi/10.2800/786656

Eurostat (2014). GEOSTAT 2011 grid dataset. Population distribution dataset (http://ec.europa.eu/eurostat/web/gisco/geodata/reference-data/population-distribution-demography) accessed 29 November 2022.

Goovaerts, P. (1997). Geostatistics for natural resources evaluation. Oxford University Press.

Hersbach, H., Bell, B., Berrisford, P., Hirahara, S., Horányi, A., Muñoz-Sabater, J., Nicolas, J., Peubey, C., Radu, R., Schepers, D., Simmons, A., Soci, C., Abdalla, S., Abellan, X., Balsamo, G., Bechtold, P., Biavati, G., Bidlot, J., Bonavita, M., … Thépaut, J.-N. (2020). The ERA5 global reanalysis. Quarterly Journal of the Royal Meteorological Society, 146(730), 1999–2049. https://doi.org/10.1002/qj.3803

Horálek, J., Vlasáková, L., Schreiberová, M., Marková, J., Schneider, P., Kurfürst, P., Tognet, F., Schovánková, J., & Vlček, O. (2021). European air quality maps for 2019. PM10, PM2.5, Ozone, NO2 and NOx Spatial estimates and their uncertainties (p. ETC/ATNI 2021/1). European

Environment Agency - European Topic Centre on Air pollution, transport, noise, and industrial pollution.

Fagerli, H., Benedictow, A., Denby, B. R., Gauss, M., Heinesen, D. Jonson, J. E., Karlsen, K. S., Klein, H., Mortier, A., Nyíri, Á., Segers., A., Simpson, D., Tsyro, S., Veldebenito, Á., Wind, P., Aas, W., Hjellbrekke, A.-G., Solberg, S., Platt, S., Tørseth, K., Yttri, K. E.,Matthews, B., Schindlbacher, S., Ullrich, B., Wankmüller, R., Klimont, Z., Scheuschner, T., Fernandez, I. A. G., Kuenen, J. J. P. (2022). EMEP Status Report 1/2022: Transboundary particulate matter, photo-oxidants, acidifying and eutrophying components (MSC-W & CCC & CEIP & CIAM Report), Norwegian Meteorological Institute, https://emep.int/publ/reports/2022/EMEP_Status_Report_1_2022.pdf.

Friedman, C.L., Selin, N.E. (2012). Long-Range Atmospheric Transport of Polycyclic Aromatic Hydrocarbons: A Global 3-D Model Analysis Including Evaluation of Arctic Sources, Environ. Sci. Technol., 46, 17, 9501–9510.

Fu, J.S., W. Aas, C. Andersson, L. Barrie, G. R. Carmichael, A. Cole, F. Dentener, C. Galy-Lacaux, J. Geddes, S. Itahashi, M. Kanakidou, F. Paulot, D. Schwede, J. Tan, R. Vet, L. Labrador (2022). Improving estimates of sulfur, nitrogen, and ozone total deposition through multi-model and measurement-model fusion approaches. Environmental Science & Technology, https://doi.org/10.1021/acs.est.1c05929.

Ge, Y., Heal, M. R., Stevenson, D. S, Wind, P., Vieno, M. (2021). Evaluation of global EMEP MSC-W (rv4.34) WRF (v3.9.1.1) model surface concentrations and wet deposition of reactive N and S with measurements. Geoscientific Model Development 2021; Volume 14. s. 7021-7046, DOI: https://doi.org/10.5194/gmd-14-7021-2021.

Gong, S. L., Huang, P., Zhao, T. L., Sahsuvar, L., Barrie, L. A., Kaminski, J. W., Li, Y. F., and Niu, T. (2007). GEM/POPs: a global 3-D dynamic model for semi-volatile persistent organic pollutants – 1. Model description and evaluations, Atmos. Chem. Phys., 7, 4001–4013, http://www.atmos-chem-phys.net/7/4001/2007/.

Gusev, A., Rozovskaya, O., Shatalov, V. (2007). Modelling POP long-range transport and contamination levels by MSCE-POPmodel, EMEP/MSC-E Technical Report 1/2007 (https://msceast.org/reports/1_2007.pdf).

Gusev A., Mantseva E., Shatalov V., Strukov B. (2005). Regional Multicompartment Model MSCE-POP. EMEP/MSC-E Technical Report 5/2005 (https://emep.int/publ/reports/5_2005.zip).

Gräler B, Pebesma E, Heuvelink G (2016). Spatio-Temporal Interpolation using gstat. The R Journal, 8, 204-218. https://journal.r-project.org/archive/2016/RJ-2016-014/index.html

Hansen, K. M., Christensen, J. H., Brandt, J., Frohn, L. M., and Geels, C. (2004). Modelling atmospheric transport of α-hexachlorocyclohexane in the Northern Hemispherewith a 3-D dynamical model: DEHM-POP, Atmos. Chem. Phys., 4, 1125–1137, https://doi.org/10.5194/acp-4-1125-2004.

Hiemstra, P., Pebesma, E., Twenhöfel, C., Heuvelink, G. (2008). Real-time automatic interpolation of ambient gamma dose rates from the Dutch Radioactivity Monitoring Network. Computers & Geosciences. DOI: http://dx.doi.org/10.1016/j.cageo.2008.10.011.

Huang, P., Gong, S. L., Zhao, T. L., Neary, L., and Barrie, L. A. (2007). GEM/POPs: a global 3-D dynamic model for semi-volatile persistent organic pollutants – Part 2: Global transports and budgets of PCBs, Atmos. Chem. Phys., 7, 4015–4025, http://www.atmos-chem-phys.net/7/4015/2007/.

Ilyin I., N.Batrakova, A.Gusev, M.Kleimenov, O.Rozovskaya, V.Shatalov, I.Strizhkina, O.Travnikov, K.Breivik, H.L.Halvorsen, P.B.Nizzetto, K.A.Pfaffuffer, W.Aas, K.Mareckova, S.Poupa, R.Wankmueller, B.Ullrich, A.Degorska (2021), Heavy metals and POPs: Pollution assessment of toxic substances on regional and global scales. EMEP Status Report 2/2021 (https://msceast.org/reports/2_2021.pdf).

Ilyin I., Degorska, A., Pandolfi M., Vana, M. (2018). Detailed assessment of heavy metal and POP pollution in the EMEP countries: Poland Part II. EMEP/MSC-E Technical Report 5/2018 https://www.msceast.org/reports/5_2018.pdf.

Jonson, J. E., Borken-Kleefeld, J., Simpson, D., Nyíri, A., Posch, M., and Heyes, C. (2017). Impact of excess NOx emissions from diesel cars on air quality, public health and eutrophication in Europe, Environ. Res. Lett., 12, 094017, https://doi.org/10.1088/1748-9326/aa8850.

Jonson J. E. and Travnikov O. (Eds.). (2010). Development of the EMEP global modeling framework: Progress report. Joint MSC-W/MSC-E Report (/reports/1_2010.pdf). EMEP/MSC-E Technical Report 1/2010.

Karl, M., Svendby, T., Walker, S.-E., Velken, A.S., Castell, N., Solberg, S. (2015). Modelling atmospheric oxidation of 2-aminoethanol (MEA) emitted from post-combustion capture using WRF-Chem. Sci. Total Environ., 527-528, 185-202. doi:10.1016/j.scitotenv. 2015.04.108.

Karl, M., Jonson, J. E., Uppstu, A., Aulinger, A., Prank, M., Sofiev, M., Jalkanen, J.-P., Johansson, L., Quante, M., and Matthias, V. (2019). Effects of ship emissions on air quality in the Baltic Sea region simulated with three different chemistry transport models, Atmos. Chem. Phys., 19, 7019–7053, https://doi.org/10.5194/acp-19-7019-2019.

Khosravi, Y., Balyani, S. (2019). Spatial Modeling of Mean Annual Temperature in Iran: Comparing Cokriging and Geographically Weighted Regression. Environ Model Assess 24, 341–354. https://doi.org/10.1007/s10666-018-9623-5.

Kaminski, J. W., Struzewska, J., Durka, P., Jeleniewicz, G., and Kawka, M. (2020). Spatial and temporal variability of benzo[a]pyrene over Poland based on modelling and observations, EGU General Assembly 2020, Online, 4–8 May 2020, EGU2020-16878, https://doi.org/10.5194/egusphere-egu2020-16878.

Kaminski, J. W., Neary, L., Struzewska, J., McConnell, J. C., Lupu, A., Jarosz, J., Toyota, K., Gong, S. L., Côté, J., Liu, X., Chance, K., and Richter, A. (2008). GEM-AQ, an on-line global multiscale chemical weather modelling system: model description and evaluation of gas phase chemistry processes, Atmos. Chem. Phys., 8, 3255–3281, https://doi.org/10.5194/acp-8-3255-2008.

Kaminski J.W. and Struzewska, J. (2013). High resolution operational air quality forecast for Poland and Central Europe with the GEM-AQ model - EcoForecast System, EGU General Assembly 2013, held 7-12 April, 2013 in Vienna, Austria, id. EGU2013-10197.

Lammel, G., Feichter, J., Leip, A. (2001). Long-range transport and global distribution of semivolatile organic compounds: A case study on two modern agrochemicals. Report Max Planck Institute for Meteorology No. 324, Hamburg.

MacLeod, M., H. von Waldow, P. Tay, J. M. Armitage, H. Wohrnschimmel, W. J. Riley, T. E. McKone and K. Hungerbuhler (2011). BETR global - A geographically-explicit global-scale multimedia contaminant fate model, Environ. Pollut., 159(5), 1442–1445, DOI: 10.1016/j.envpol.2011.01.038.

Marécal, V., Peuch, V.-H., Andersson, C., Andersson, S., Arteta, J., Beekmann, M., Benedictow, A., Bergström, R., Bessagnet, B., Cansado, A., Chéroux, F., Colette, A., Coman, A., Curier, R. L., Denier van der Gon, H. A. C., Drouin, A., Elbern, H., Emili, E., Engelen, R. J., Eskes, H. J., Foret, G., Friese, E., Gauss, M., Giannaros, C., Guth, J., Joly, M., Jaumouillé, E., Josse, B., Kadygrov, N., Kaiser, J. W., Krajsek, K., Kuenen, J., Kumar, U., Liora, N., Lopez, E., Malherbe, L., Martinez, I., Melas, D., Meleux, F., Menut, L., Moinat, P., Morales, T., Parmentier, J., Piacentini, A., Plu, M., Poupkou, A., Queguiner, S., Robertson, L., Rouïl, L., Schaap, M., Segers, A., Sofiev, M., Tarasson, L., Thomas, M., Timmermans, R., Valdebenito, Á., van Velthoven, P., van Versendaal, R., Vira, J., and Ung, A. (2015). A regional air quality forecasting system over Europe: the MACC-II daily ensemble production, Geosci. Model Dev., 8, 2777–2813, https://doi.org/10.5194/gmd-8-2777-2015.

Matheron, G. (1963). Principles of geostatistics. Econ. Geol., 58, 1246-1266.

Meijer, J. R., Huijbregts, M. A. J., Schotten, K. C. G. J., & Schipper, A. M. (2018). Global patterns of current and future road infrastructure. Environmental Research Letters, 13(6), 064006. https://doi.org/10.1088/1748-9326/aabd42

McFiggans, G., Mentel, T. F.,Wildt, J., Pullinen, I., Kang, S., Kleist, E., Schmitt, S., Springer, M., Tillmann, R., Wu, C., Zhao, D., Hallquist, M., Faxon, C., Le Breton, M., Hallquist, Å. M., Simpson, D., Bergström, R., Jenkin, M. E., Ehn, M., Thornton, J. A., Alfarra, M. R., Bannan, T. J., Percival, C. J., Priestley, M., Topping, D., and Kiendler-Scharr, A. (2019). Secondary organic aerosol reduced by mixture of atmospheric vapours, Nature, 565, 587–593, https://doi.org/10.1038/s41586-018-0871-y.

Muñoz-Sabater, J., Dutra, E., Agustí-Panareda, A., Albergel, C., Arduini, G., Balsamo, G., Boussetta, S., Choulga, M., Harrigan, S., Hersbach, H., Martens, B., Miralles, D. G., Piles, M., Rodríguez-Fernández, N. J., Zsoter, E., Buontempo, C., & Thépaut, J.-N. (2021). ERA5-Land: A state-of-the-art global reanalysis dataset for land applications. Earth System Science Data, 13(9), 4349–4383. https://doi.org/10.5194/essd-13-4349-2021

Oliver, M.A. and Webster, R. A tutorial guide to geostatistics (2014). Computing and modelling variograms and kriging,CATENA, 113,56-69, https://doi.org/10.1016/j.catena.2013.09.006.

O'Neill, N. T., Campanelli, M., Lupu, A., Thulasiraman, S., Reid, J. S., Aub´e, M., Neary, L., Kaminski, J. W., and McConnell, J. C. (2006). Evaluation of the GEM–AQ air quality model during the Québec smoke event of 2002: Analysis of extensive and intensive optical disparities, Atmos. Environ., 40, 3737–3749.

Pebesma, E.J. (2004). Multivariable geostatistics in S: the gstat package. Computers & Geosciences, 30, 683-691.

Roeckner, E., Oberhuber, J.M., Bacher, A., Christoph, M., Kirchner, I. (1996). ENSO variability and atmospheric response in a global coupled atmosphere–ocean GCM. Clim. Dyn. 12, 737–754.

Schwede, D. B., Lear, G. G. (2014). A Novel Hybrid Approach for Estimating Total Deposition in the United States. Atmos. Environ. 2014, 92, 207–220. https://doi.org/10.1016/j.atmosenv.2014.04.008.

Schwede, D., Cole, A., Vet, R., Lear, G. (2019). On-Going U.S.-Canada Collaboration on Nitrogen and Sulfur Deposition on Nitrogen and Sulfur Deposition. The Magazine for Environmental Managers, June, 1-5.

Simpson, D., Benedictow, A., Berge, H., Bergström, R., Emberson, L. D., Fagerli, H., Flechard, C. R., Hayman, G. D., Gauss, M., Jonson, J. E., Jenkin, M. E., Nyíri, A., Richter, C., Semeena, V. S., Tsyro, S., Tuovinen, J.-P., Valdebenito, Á., and Wind, P. (2012). The EMEP MSC-W chemical transport model – technical description, Atmos. Chem. Phys., 12, 7825–7865, https://doi.org/10.5194/acp-12-7825-2012.

Skamarock, W. C., and Klemp, J. B. (2008). A time-split nonhydrostatic atmospheric model for weather research and forecasting applications, J. Comput. Phys., 227 (7), 3465-3485, 10.1016/j.jcp.2007.01.037.

Struzewska, J., Kaminski, J.W. (2010). Semi-operational air quality forecast for Poland and Central Europe with the GEM-AQ model, 13th Conference on Harmonisation within Atmospheric Dispersion Modelling for Regulatory Purposes (https://www.harmo.org/Conferences/Proceedings/_Paris/publishedSections/H13-145-abst.pdf).

Struzewska, J. and Kaminski, J. W. (2008). Formation and transport of photooxidants over Europe during the July 2006 heat wave – observations and GEM–AQ model simulations, Atmos. Chem. Phys., 8, 721–736, http://www.atmos-chem-phys.net/8/721/2008/.

Tarrasón L. and Gusev A. (2008). Towards the development of a common EMEP global modeling framework. MSC-W Technical Report 1/2008 (https://emep.int/publ/reports/2008/emep_technical_1_2008.pdf).

Travnikov O., Angot H., Artaxo P., Bencardino M., Bieser J., D'Amore F., Dastoor A., De Simone F., Diéguez M. D. C., Dommergue A., Ebinghaus R., Feng X. B., Gencarelli C. N., Hedgecock I. M., Magand O., Martin L., Matthias V., Mashyanov N., Pirrone N., Ramachandran R., Read K. A., Ryjkov A., Selin N. E., Sena F., Song S., Sprovieri F., Wip D., Wängberg I., and Yang X. (2017). Multi-model study of mercury dispersion in the atmosphere: atmospheric processes and model evaluation, Atmos. Chem. Phys., 17, 5271-5295, doi:10.5194/acp-17-5271-2017.

Travnikov O. and Jonson J. E. (Eds.). (2011). Global scale modelling within EMEP: Progress report. EMEP/MSC-E Technical Report 1/2011 (https://emep.int/publ/reports/reports/1_2011.pdf).

Travnikov O., J.E. Jonson, A.S Andersen, M. Gauss, A. Gusev, O. Rozovskaya, D. Simpson, V. Sokovykh, S. Valiyaveetil and P. Wind (2009). Development of the EMEP global modelling framework: Progress report. Joint MSC-E/MSC-W Report.EMEP/MSC-E Technical Report 7/2009 (https://emep.int/publ/reports/7_2009.pdf).

Travnikov O. and I.Ilyin (2005). Regional Model MSCE-HM of Heavy Metal Transboundary Air Pollution in Europe. EMEP/MSC-E Technical Report 6/2005 (https://emep.int/publ/reports/6_2005.zip), p.59.

van Geffen, J., Boersma, K. F., Eskes, H., Sneep, M., ter Linden, M., Zara, M., & Veefkind, J. P. (2020). S5P TROPOMI NO2 slant column retrieval: Method, stability, uncertainties and comparisons with OMI. Atmospheric Measurement Techniques, 13(3), 1315–1335. https://doi.org/10.5194/amt-13-1315-2020

Veefkind, J. P., Aben, I., McMullan, K., Förster, H., de Vries, J., Otter, G., Claas, J., Eskes, H. J., de Haan, J. F., Kleipool, Q., van Weele, M., Hasekamp, O., Hoogeveen, R., Landgraf, J., Snel, R., Tol, P., Ingmann, P., Voors, R., Kruizinga, B., … Levelt, P. F. (2012). TROPOMI on the ESA Sentinel-5 Precursor: A GMES mission for global observations of the atmospheric composition for climate, air quality and ozone layer applications. Remote Sensing of Environment, 120, 70–83. https://doi.org/10.1016/j.rse.2011.09.027

Wackernagel, H. (2013). Multivariate geostatistics: An introduction with applications. Springer Science & Business Media.

Wania, F., Breivik, K., Persson N. J. and McLachlan, M. S. (2006). CoZMo-POP 2 - A fugacity-based dynamic multicompartmental mass balance model of the fate of persistent organic pollutants, Environ. Model. Software, 21(6), 868–884, DOI: 10.1016/j.envsoft.2005.04.003.

Wesely, M. (1989). Parametrizations of surface resistance to gaseous dry deposition in regional scale, numerical models. Atmos. Environ., 23:1293–1304.

Zhang, L., Brook, J. R., and Vet, R. (2003). A revised parameterization for gaseous dry deposition in air-quality models, Atmos. Chem. Phys., 3, 2067–2082, https://doi.org/10.5194/acp-3-2067-2003.

Appendix A

R script used for kriging the Polish precipitation data

```
# Script for kriging polish precipitation data.
# Prepare concentration data as
#calcualte emepx emepy for lon lat for polish sites
# Constraining the variograms with nugget = 0 and range = 5

library(tidyverse) # wrangling tabular data and plotting
library(sf) # processing spatial vector data - the easy way
library(sp) # processing spatial vector data - the way gstat needs it
library(raster) # processing spatial raster data.
library(gstat)   # The most popular R-Package for Kriging (imho)
library(automap) # Automatize some (or all) parts of the gstat-workflow
library(patchwork) # packages to make pretty plots
library(viridis)# packages to make pretty plots


#Defining a target grid, include the file with emep50 grid
grid_emep50 <- read.table("C/emepgrid_pl.csv", sep = ",",header = TRUE)
df_grid <- st_as_sf(grid_emep50, coords = c("emep50i", "emep50j")) %>%
  cbind(st_coordinates(.)) #Convert to {sf}

# making our grid work for gstat
grd_sp <- as(df_grid, "Spatial") # converting to {sp} format
gridded(grd_sp) <- TRUE            # informing the object that it is a grid
grd_sp <- as(grd_sp, "SpatialPixels") # specifying what kind of grid

#Read the file with conc of 2020
df_2020 <- read.table("C/conc2020.csv", sep = ",",header = TRUE)

# make a loop to do all compunds
for (comp in c('so4','no3','nh4','pb','cd')){

  df = df_2020[c("emepx", "emepy",comp)]
  colnames(df)[3]  <- "conc"    # change column name for x column
  df <- df[complete.cases(df), ] # delete rows with NANs

  # Convert to {sf} because that is the best way to store spatial points
  df_sf <- st_as_sf(df, coords = c("emepx", "emepy")) %>%
    cbind(st_coordinates(.))

  #Creating a Variogram
  vario <- gstat::variogram(
    conc~1,
    as(df_sf, "Spatial") # switch from {sf} to {sp}
  )

  #Fit variogram model, fix Nugget and Range
  fit.variog<- automap::autofitVariogram(conc~1, as(df_sf, "Spatial"), fix.values = c(0,4,NA),)

  #Plot variogram with fit on screen
  plot(vario, fit.variog, pch=19, cex = 2, lwd = 3)
  plot(automap::autofitVariogram(conc~1, as(df_sf, "Spatial"),fix.values = c(0,4,NA),), pch=19, cex = 2, lwd = 3)

  #Export variogram plot
  png(paste("C:/",comp,"_2020_vario.png",sep=""))
  plot(automap::autofitVariogram(conc~1, as(df_sf, "Spatial"),fix.values = c(0,4,NA),), pch=19, cex = 2, lwd = 3)
  dev.off()
```

```
# Ordinary Kriging (OK)
OK <- krige(
  conc~1,                          # conc is our variable and "~1" means "depends on mean"
  as(df_sf, "Spatial"),            # input data in {sp} format
  grd_sp,                          # locations to interpolate at
  model = fit.variog               # the variogram model fitted above
)

# IDW
IDW <- idw(
  conc~1,                          # conc is our variable and "~1" means "depends on mean"
  as(df_sf, "Spatial"),            # input data in {sp} format
  grd_sp,                          # locations to interpolate at
)

# A function to plot rasters
plot_my_gstat_output <- function(raster_object, object_name){

  df <- rasterToPoints(raster_object) %>% as_tibble()
  colnames(df) <- c("emepx", "emepy", "conc")

  ggplot(df, aes(x = emepx, y = emepy, fill = conc)) +
    geom_raster() +
    ggtitle(label = object_name) +
    scale_fill_viridis(option = "H") +
    theme_void() +
    theme(
      plot.title = element_text(hjust = 0.5)
    )
}

# plot observations
p_obs <- ggplot(
  data = df,
  mapping = aes(x = emepx, y = emepy, color = conc)
) +
  geom_point(size = 5) +
  ggtitle(label = "Observations") +
  scale_color_viridis(option = "H") +
  theme_void() +
  theme(
    plot.title = element_text(hjust = 0.5)
  )

p_OK <- plot_my_gstat_output(raster(OK), paste("Ordinary Kriging",comp))
p_IDW <- plot_my_gstat_output(raster(IDW), paste("IDW"))

#plot observations and kriging together
print((p_OK + p_IDW + p_obs) + plot_layout(guides = 'collect'))


#Export plot
png(paste("C: /maps",comp,"_2020_krige.png",sep=""))
p_OK <- plot_my_gstat_output(raster(OK), paste("Ordinary Kriging",comp))
p_IDW <- plot_my_gstat_output(raster(IDW), paste("IDW"))
print((p_OK+ p_IDW + p_obs) + plot_layout(guides = 'collect'))
dev.off()

#Export csv file of kriged observation
write.csv(p_OK[["data"]],(paste("C:/",comp,"_emep50_2020_krige.csv",sep="")),row.names = TRUE)
write.csv(p_IDW[["data"]],(paste("C:/",comp,"_emep50_2020_IDW.csv",sep="")),row.names = TRUE)
}
```

NILU – Norwegian Institute for Air Research

NILU – Norwegian Institute for Air Research is an independent, non-profit institution established in 1969. Through its research NILU increases the understanding of climate change, of the composition of the atmosphere, of air quality and of hazardous substances. Based on its research, NILU markets integrated services and products within analysing, monitoring and consulting. NILU is concerned with increasing public awareness about climate change and environmental pollution.

NILU's values: *Integrity - Competence - Benefit to society*
NILU's vision: *Research for a clean atmosphere*

NILU – Norwegian Institute for Air Research
P.O. Box 100, NO-2027 KJELLER, Norway

E-mail: nilu@nilu.no
http://www.nilu.no

ISBN: 978-82-425-3108-7
ISSN: 2464-3327

Norsk institutt for luftforskning
Norwegian Institute for Air Research